Temporal variation of oxidative potential of water soluble components of ambient PM$_{2.5}$ measured by dithiothreitol (DTT) assay

Jingpeng Wang [a], Xin Lin [b], Liping Lu [a,c], Yujie Wu [a,c], Huanxin Zhang [d], Qi Lv [a], Weiping Liu [a,c], Yanlin Zhang [b], Shulin Zhuang [a,e,*]

[a] College of Environmental and Resource Sciences, Zhejiang University, Hangzhou 310058, China
[b] Yale-NUIST Center on Atmospheric Environment, Nanjing University of Information Science and Technology, Nanjing 210044, China
[c] Research Center for Air Pollution and Health, Zhejiang University, Hangzhou 310058, China
[d] College of Marine Life Sciences, Ocean University of China, Qingdao 266003, China
[e] The First Affiliated Hospital College of Medicine, Zhejiang University, Hangzhou 310003, China

HIGHLIGHTS

- Ambient PM$_{2.5}$ showed significant seasonal variations in Hangzhou city in 2017.
- The annual mean of volume-normalized DTT activity (DTTv) was 0.62 ± 0.24 nmol/min/m^3.
- The mass-normalized DTT activity (DTTm) showed seasonal and diurnal variations.
- The oxidative potential (OP) of PM$_{2.5}$ was dominated mainly by the components rather than mass concentration.
- Secondary inorganic aerosol (SIA) species were correlated prominently with DTTv (p < 0.05).

GRAPHICAL ABSTRACT
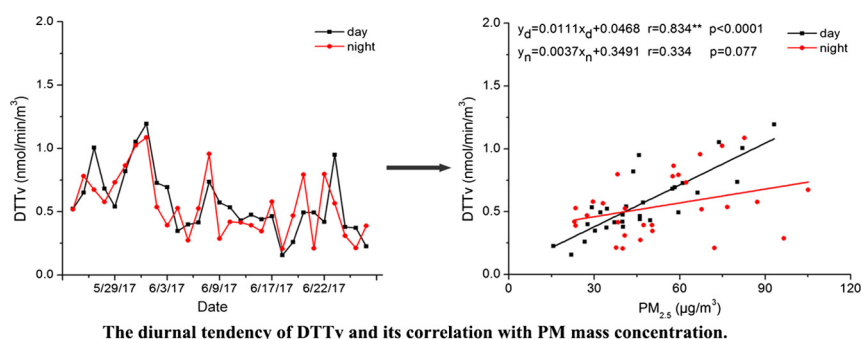
The diurnal tendency of DTTv and its correlation with PM mass concentration.

ABSTRACT

The exposure to ambient fine particulate matter (PM$_{2.5}$) can induce oxidative stress, contributing to global burden of diseases. The evaluation of the oxidative potential (OP) of PM$_{2.5}$ is thus critical for the health risk assessment. We collected ambient PM$_{2.5}$ samples in Hangzhou city, China for four consecutive quarters in the year 2017 and investigated the oxidation property of PM$_{2.5}$ components by the dithiothreitol (DTT) assay. The annual mean of ambient PM$_{2.5}$ mass concentrations in 2017 was 63.05 μg m^{-3} (median: 57.34, range: 6.67–214.33 μg m^{-3}) with the significant seasonal variations ranking as winter > spring > summer > autumn. Secondary inorganic aerosol (SIA) species including SO$_4^{2-}$, NO$_3^-$ and NH$_4^+$ totally account for >50% of PM$_{2.5}$ mass. The annual mean volume-normalized DTT activity (DTTv) showed a relatively high value of 0.62 nmol/min/m^3 (median: 0.62, range: 0.11–1.66 nmol/min/m^3) and DTTv of four seasons was roughly at the same level, indicating a high annual exposure level of ambient PM$_{2.5}$. SIA species were correlated well with the corresponding DTTv and showed significant diurnal variations with strong or moderate correlations at day and weak correlations at night, suggesting strong secondary formation in daytime with contribution to the particulate OP. The annual mean mass-normalized DTT activity (DTTm) had a relatively low value of 6.39 pmol/min/μg (median: 5.63, range: 1.99–22.70 pmol/min/μg), indicating low intrinsic oxidative toxicity. The DTTm of four seasons ranked as autumn > winter > spring > summer, indicating seasonal variations of the DTT-active components. The PM$_{2.5}$

* Corresponding author.
E-mail address: shulin@zju.edu.cn (S. Zhuang).

mass concentration is more related to exposure levels than intrinsic properties of components, while OP is determined by the components rather than $PM_{2.5}$ mass concentration. Our results provide an insight into reactive oxygen species-induced health risk of $PM_{2.5}$ exposure and decision for subsequent emission control.

1. Introduction

The fine particulate matter ($PM_{2.5}$) contributes significantly to the ambient air pollution occurred frequently in many regions and countries, arising public health concern. Exposure to $PM_{2.5}$ contributes to the global burden of diseases and $PM_{2.5}$ was ranked among the top five global mortality risk factors (Cohen et al., 2017). Numerous epidemiological studies have revealed the association between $PM_{2.5}$ and increasing morbidity and mortality from various diseases, including cardiovascular diseases, respiratory system disorders, and lung cancer (Cao et al., 2012; Sun et al., 2010). The exposure to fine PM with a 10-$\mu g/m^3$ elevation was reported to cause 8% to 18% increase in mortality risk for ischemic heart disease, dysrhythmias, heart failure, and cardiac arrest (Pope et al., 2004). The long-term residential exposure to air pollution with a ten-unit increase in $PM_{2.5}$ ($\mu g/m^3$) led to the increase of 1.29 (95% confidence interval = 0.95–1.76) for lung cancer incidence in eight Canadian provinces from 1994 to 1997 (Hystad et al., 2013). Although the underlying pathological mechanisms for these diseases are yet incompletely understood, $PM_{2.5}$-induced oxidative stress is considered one of the major biochemical pathways (Rui et al., 2016; Valavanidis et al., 2013). The exposure to $PM_{2.5}$ may stimulate cells to produce excessive reactive oxygen species (ROS) and disturb redox homeostasis, thereby triggering a cascade of downstream episodes such as systemic inflammation, DNA damage and cell death (Becker et al., 2005; Soberanes et al., 2009; Vattanasit et al., 2014; Xu et al., 2018).

The oxidative potential (OP) of $PM_{2.5}$ is a versatile indicator suitable for the evaluation of the oxidation property of PM components (Crobeddu et al., 2017; Perrone et al., 2016). Determination of ambient fine particulate OP can be used as a promising and integrative metric for preliminary screening. ROS were produced through transferring electron from cellular reductants, such as NADPH, to molecular oxygen (Kumagai et al., 1997; Liu et al., 2017). Dithiothreitol (DTT) was used reportedly as a substitute of cellular reductants and chemical components of $PM_{2.5}$ can catalyze electronic transport from DTT to oxygen, generating superoxide radical. The ambient particulate OP can be evaluated by the determination of DTT consumption rates (Cho et al., 2005; Kumagai et al., 2002). The measured volume-normalized DTT activities (DTTv) and mass-normalized DTT activities (DTTm) can facilitate to characterize the exposure-relevant levels and intrinsic properties of $PM_{2.5}$. This cell-free DTT assay is used frequently to measure the ambient particulate OP with the advantages of fast results reading and strong environmental controllability (Rattanavaraha et al., 2011; Vreeland et al., 2017).

The DTT assay can effectively assess the temporospatial variation trend of ambient particulate OP at long-term, low-dose exposure levels. Such seasonal and diurnal variation is crucial for the prediction of ROS-induced regional health risks. The significant seasonal variations of ambient particulate OP were observed in Atlanta and Los Angeles Basin that higher DTT activities occurred in colder months than in warmer periods (Fang et al., 2015b; Saffari et al., 2014). The significant diurnal variation was also observed in coastal cities of the Bohai Sea with higher DTT activities in summer nighttime than in daytime (Liu et al., 2018). The temporospatial variation of OP is contributed by different components. Certain metals and organic components were reported to be associated with ROS or OP

(Fang et al., 2015a; Verma et al., 2015). Copper and manganese were the most DTT-active compounds among the soluble transition metals of $PM_{2.5}$, and quinones were moderately contributed to DTT loss (Charrier and Anastasio, 2012). Secondary organic aerosol was also reported to be a major contributor associated with DTT activity (Ma et al., 2018; Tuet et al., 2017). Secondary inorganic aerosol (SIA, including SO_4^{2-}, NO_3^- and NH_4^+) contributes a large amount of $PM_{2.5}$, however their relations to the OP of $PM_{2.5}$ need to be clarified (Jansen et al., 2014; Xu et al., 2017). SIA-abundance ambient PM may produce acidic environment, possibly inducing oxidative stress and inflammation through synergistic action with other components (e.g. transition metals) (Fang et al., 2017a). Therefore, it is necessary to emphasize the relation of SIA to ambient particulate OP, which is essential to better assess the adverse health effects of different $PM_{2.5}$ components.

In the present study, we collected ambient $PM_{2.5}$ samples in Hangzhou city, China for four consecutive quarters in 2017 and monitored online their components. The seasonal and diurnal variations of the exposure-relevant level and intrinsic properties of $PM_{2.5}$ were investigated by the measurements of DTTv and DTTm via the DTT assay. The relation of SIA to the observed OP of ambient $PM_{2.5}$ was further identified. Our results indicated ROS-induced external exposure risk at long term and deciphered the components contributing to the adverse effect. Such information is critical to the elucidation of downstream molecular mechanism and beneficial to subsequent emission control decisions.

2. Materials and methods

2.1. Site description and $PM_{2.5}$ sampling

The $PM_{2.5}$ samples were collected at the environmental monitoring station of Zhejiang University in Hangzhou city, China (30.31°N, 120.08°E). There is a two-way six-lane highway about 700 m away from the north side of the station and a construction site 500 m away from the west site. The combined influence of residential, traffic, and construction emissions makes it as a well representative of urban emission levels. The ambient air $PM_{2.5}$ sampler was put on the roof of the station, about 5 m above ground level without visible tall buildings and pollution source around. Ambient $PM_{2.5}$ samples were continuously collected in winter (December 20, 2016–January 20, 2017), spring (March 20, 2017 to April 20, 2017), summer (May 25, 2017–June 29, 2017), and autumn (October 9, 2017–November 11, 2017). The sampling collection last for 23 h each day during winter and spring, while in summer and autumn, sampling times for day and night samples were 09:00 to 20:30 h and 21:00 to 08:30 h, respectively. The meteorological data during sampling periods were listed in Table 1.

A high-volume sampler (model KC-1000, Laoshan Mountain Electronic Instrument Factory Co., Ltd.) equipped with a $PM_{2.5}$ selective-inlet head was employed to collect particles with the nominal flow rate of 1.05 m^3/min using prebaked 8 × 10 inch quartz fiber filters (Peta Instrument Co., Ltd., Guangzhou, China). The filters were equilibrated (72 h at 39% RH, room T) and weighed with a microbalance (100 μg precision) before and after the sampling and all sampled filters were immediately wrapped in aluminum foil and stored in the refrigerator at −20 °C until analysis. The blank filters were prepared by operating the sampler for 10s at the beginning

Table 1
The concentration of PM$_{2.5}$ and relevant meteorological data in four seasons of 2017.[a]

Item	Component	Winter (n = 32)	Spring (n = 32)	Summer (n = 29)	Autumn (n = 31)
PM$_{2.5}$	PM$_{2.5}$	88.83, 76.23, 26.83–214.33	66.02, 63.48, 22.67–135.12	50.30, 45.83, 19.50–93.54	47.03, 47.79, 7.89–109.54
Meteorological data	T (°C)	6.9, 6, 2–12	14.2, 13.5, 8–21	24.1, 24, 21.5–28.5	17.4, 17.5, 12.5–28
	BP (kPa)	102.2, 102.2, 100.9–103.4	101.2, 101.2, 99.9–102.2	100.3, 100.4, 99.7–100.9	102.2, 102.2, 101.5–103.2
	RH (%)	82, 81, 42–98	76, 81, 46–95	73, 72, 43–96	72, 75, 40–88
	WS (m/s)	2.2, 2.0, 0.1–8.2	4.1, 3.8, 1.5–10.2	3.0, 2.6, 0.9–5.6	3.0, 3.1, 1.1–5.7
	VIS (km)	4.2, 3.1, 0.3–13.6	7.1, 7.4, 1.7–17.6	10.6, 9.3, 3.8–22.0	10.9, 10.5, 4.8–16.1

[a] Data were obtained from the central meteorological observatory (http://www.nmc.cn/) and represented as mean, median and range.

and end of each sampling period and totally eight field filter blanks were used to guarantee the quality of PM measurements and analysis.

2.2. Filter extraction protocol

The filters were punched with a 16 mm-diameter hole for winter and spring samples or a 25 mm-diameter hole for summer and autumn samples. The separated circular filters were soaked in 10 mL of deionized water (18.2 MΩ, Millipore, Bedford, MA) and were further sonicated by an Ultrasonic Cleaner (model KQ-400E, Kunshan Ultrasonic Instrument Co., Ltd., Jiangsu, China) for 30 min. The extracts were filtered to remove insoluble components and any filter fibers using 0.45 μm PTFE syringe filters (Whatman, USA).

2.3. Real-time online monitoring

The concentrations of PM$_{2.5}$ and sulfur dioxide (SO$_2$), nitrogen dioxide (NO$_2$), carbon monoxide (CO), and ozone (O$_3$), were measured by a colocated real-time monitor equipped with the module TEOM 1405-PM$_{2.5}$, 43i-SO$_2$, 42i-NO$_2$, 48i-CO and 49i-O$_3$ (Thermo Fisher Scientific, USA). In total eight major water-soluble inorganic ions, including chlorine (Cl$^-$), nitrate (NO$_3^-$), sulfate (SO$_4^{2-}$), ammonium (NH$_4^+$), sodium (Na$^+$), potassium (K$^+$), magnesium (Mg^{2+}), and calcium (Ca^{2+}), were obtained from a colocated aerosol real-time online monitor (MARGA, model ADI 2080, Metrohm Applikon, Holland). The instruments were routinely calibrated for the quality control before the measurements.

2.4. Oxidative potential (OP) measurement

The DTT assay was performed to evaluate OP of particles following reported protocols (Text S1) (Charrier and Anastasio, 2012; Cho et al., 2005). The remaining DTT reacts with 5,5′-dithiobis-2-nitrobenzoic acid (DTNB) and generates 2-nitro-5-thiobenzoic acid (TNB) with a high extinction coefficient at 412 nm.

For the OP measurement, 4.55 mL potassium phosphate buffer (0.1 M, pH = 7.4, Chelex 100 resin treatment) and 1.75 mL PM extract sample (or blank and positive control) were added in a 10 mL glass centrifuge vial and the mixture was incubated at 37 °C for 5 min. The DTT (1 mM) of 0.7 mL was added to initiate the oxidation reaction. After the incubation of 0, 10, 20 and 30 min, a 0.5 mL aliquot from the reaction mixture was transferred to another centrifuge tube preloaded with 0.5 mL TCA (10% w/v) to terminate the reaction. 2 mL Tris-Base (0.4 M Tris with 20 mM EDTA, pH = 8.9) and 50 μL DTNB (10 mM) were then added to the aliquot mixture and DTT can react with DTNB to form TNB. After 5 min incubation at room temperature, the absorbance spectrum was measured by a UV–Visible spectrometer (Jasco V-750 Spectrophotometer, JASCO Corporation, Japan) at 412 nm. The deionized water and 9,10-phenanthrenequinone (PQN, 0.24 μM) were used for blank and positive control, respectively.

The absorbance was calibrated with known concentrations (1, 5, 10, 25, 50, 75 and 100 μM) of DTT, and the calibration curve was used to calculate the residual amount of DTT in the mixture (Fig. S1). The DTT consumption rate was normalized by the total volume of air passing through the filter (volume-normalized DTT activities, DTTv) and the

total mass of PM participating in the reaction (mass-normalized DTT activities, DTTm) following a reported protocol (Fang et al., 2017b).

$$DTT_v \left(nmol \; min^{-1} m^{-3} \right) = \frac{r_s \left(nmol \; min^{-1} \right) - r_b \left(nmol \; min^{-1} \right)}{V_t \; (m^3) \times \frac{A_h \; (cm^2)}{A_t \; (cm^2)} \times \frac{V_s \; (mL)}{V_e \; (mL)}}$$

$$DTT_m \left(nmol \; min^{-1} \; ug^{-1} \right) = \frac{r_s \left(nmol \; min^{-1} \right) - r_b \left(nmol \; min^{-1} \right)}{M_t \; (ug) \times \frac{A_h \; (cm^2)}{A_t \; (cm^2)} \times \frac{V_s \; (mL)}{V_e \; (mL)}}$$

where r_s and r_b are the DTT consumption rates of sample and blank, respectively. V_t and M_t are the total sampling air volume and the total particle mass (with filter blank correcting), respectively. A_h and A_t are the area of hole and total filter, respectively. V_s and V_e are the sample volume participating in reaction and extraction volume, respectively. All measurements were performed in triplicate with the filters and reagent blanks correcting. At least one blank control and one positive control were guaranteed for each test.

2.5. Statistical analysis

Seasonal and diurnal variability of aerosol OP and concentrations of individual components were analyzed by one-way analysis of variance (ANOVA) using LSD's multiple comparisons by SPSS 20.0. The correlation between OP and water-soluble components were analyzed using Spearman rank correlation coefficients (r_s) by SPSS 20.0. The significant difference is considered with p < 0.05.

3. Results and discussion

3.1. PM$_{2.5}$ mass concentration and chemical components

We monitored online the concentration of PM$_{2.5}$ for four consecutive quarters in 2017 (Fig. 1). The annual mean of PM$_{2.5}$ mass concentration
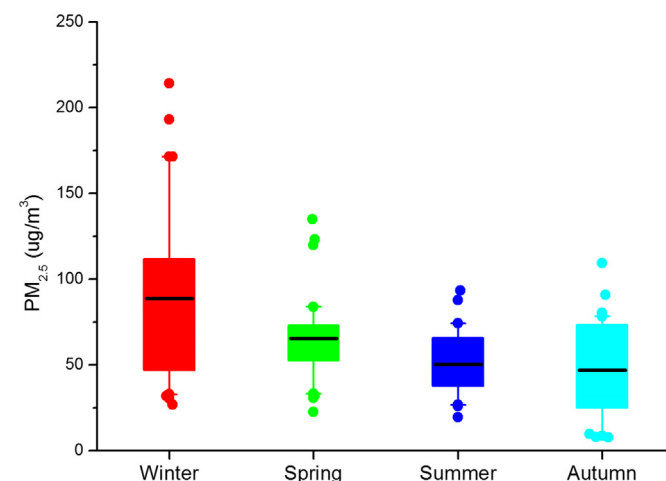
Fig. 1. Box plots of the concentrations of PM$_{2.5}$ sampled in Hangzhou city in 2017.

is 63.05 μg m^{-3} (median: 57.34, range: 6.67–214.33 μg m^{-3}), exceeding the Chinese National Ambient Air Quality Standards' Grade II at 35 μg m^{-3}. The significant seasonal variations were observed with the seasonal pattern ranking as winter (average: 88.83, median: 76.23, range: 26.83–214.33 μg m^{-3}) > spring (average: 66.02, median: 63.48, range: 22.67–135.12 μg m^{-3}) > summer (average: 50.30, median: 45.83, range: 19.50–93.54 μg m^{-3}) > autumn (average: 47.03, median: 47.79, range: 7.89–109.54 μg m^{-3}). Heavy pollution often erupted in winter with the individual values exceeding 200 μg m^{-3}. We further investigated the averaged 48-hour air mass back trajectories using the Hybrid Single-Particle Lagrangian Integrated Trajectory (HYSPLIT) model. The source of air masses in different color varied significantly in different seasons (Fig. 2). The mixed oceanic, terrestrial and local origins may partly contribute to the ambient particle concentrations. The air pollution episodes in Hangzhou were possibly the synergistic effects of regional transport and local pollution accumulation caused by increased anthropogenic emission under stagnant meteorological conditions (Li et al., 2015; Zhang et al., 2018).

We recorded the major inorganic ions (Cl$^-$, NO$_3^-$, SO$_4^{2-}$, NH$_4^+$, Na$^+$, K$^+$, Ca^{2+}, Mg^{2+}) in summer and autumn (Table S1). Secondary inorganic aerosol (SIA) species including SO$_4^{2-}$, NO$_3^-$ and NH$_4^+$ totally accounted for >50% of PM$_{2.5}$ mass and their averaged concentrations were 7.95 (median: 6.77, range: 0.72–22.71), 9.44 (median: 8.08, range: 1.09–44.21) and 5.73 (median: 5.21, range: 0.63–18.34) μg m^{-3}, respectively. SIA contributed significantly to the PM$_{2.5}$ pollution, in line with the measured PM$_{2.5}$ in 2013 (Wu et al., 2016), indicating the strong secondary formation occurred in Hangzhou. The concentration of remaining ions accounted for ~5% of PM$_{2.5}$ mass and ranked as Cl$^-$ > K$^+$ > Ca^{2+} > Na$^+$ > Mg^{2+}, showing the nonnegligible impact of biomass burning to air pollution (Xu et al., 2017).

3.2. Oxidative potential of water-soluble PM$_{2.5}$

The DTT consumption rate was calculated by the linear regression slope of the 4 time points (Fig. S2). All samples had a good linearity and parallelism (R^2 > 0.95, p < 0.05). Multiple control groups (n = 34) were performed simultaneously with PM samples to verify the reproducibility of different batches of experiments (Table S2). The average rate of positive control was 1.096 nmol/min with a coefficient of variation (CV %) of 8.6%, comparable with the reported 1.02 nmol/min at same PQN concentration (Gao et al., 2017). The CV % of all samples was within acceptable limits, indicating that the assay was highly consistent with a moderately small-scale variability (Fang et al., 2015b).

Our calculated annual mean DTTv based on one year-long period dataset (n = 124, Table S3) was 0.62 nmol/min/m^3 (median: 0.62, range: 0.11–1.66 nmol/min/m^3), higher than reported values of Beijing (mean, 0.19 nmol/min/m^3) (Liu et al., 2014), Shanghai (0.13 nmol/min/m^3) (Lyu et al., 2018), Atlanda (0.31 nmol/min/m^3) (Fang et al., 2016), Lecce (0.40 ± 0.26 nmol/min/m^3) (Chirizzi et al., 2017), and was significantly lower than that measured in Baohai Sea (0.16–14.47 nmol/min/m^3) (Liu et al., 2018) and Indo-Gangetic Plain (3.8 ± 1.4 nmol/min/m^3) (Patel and Rastogi, 2018). The measured DTTm at 6.39 pmol/min/μg (median: 5.63, range: 1.99–22.70 pmol/min/μg) was generally lower than reported values. There is a remarkable association between OP and multiple cardiorespiratory outcomes as indicated by the population-level health effects (Abrams et al., 2017; Bates et al., 2015). Our calculated relatively high annual mean DTTv and low DTTm indicate a relatively high exposure risk and low intrinsic oxidative toxicity.

The daily PM$_{2.5}$ concentrations with the corresponding water-soluble oxidative potential were further presented in time series (Fig. 3). Although the day-to-day sampling mode may reduce the diurnal variation of emission sources, there were still significant changes between adjacent days. The PM$_{2.5}$ and DTTv showed similar variation tendency (Fig. 3a, b), while the DTTm had no such pattern (Fig. 3c). Our results indicated that the exposure levels to PM$_{2.5}$ is more related to its mass concentration rather than the intrinsic properties of components, and the relevant OP is dominated mainly by the components rather than PM mass concentration. Therefore, both the mass concentration and its internal components are necessarily needed to be fully considered for comprehensive evaluation of PM toxicity.

The seasonal variability in DTTv and DTTm were further investigated (Table S4). The DTTv values at winter and autumn were roughly at the same level (p = 0.243). There is a significant mean difference of 0.127 for DTTv measured in spring and summer (p = 0.042). DTTm exhibited
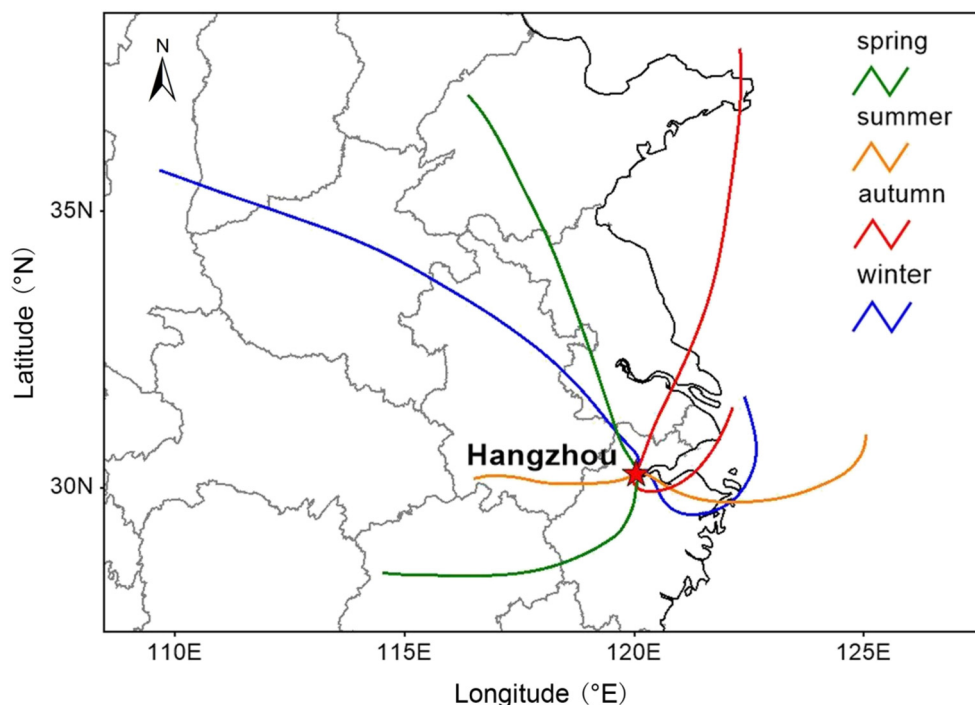

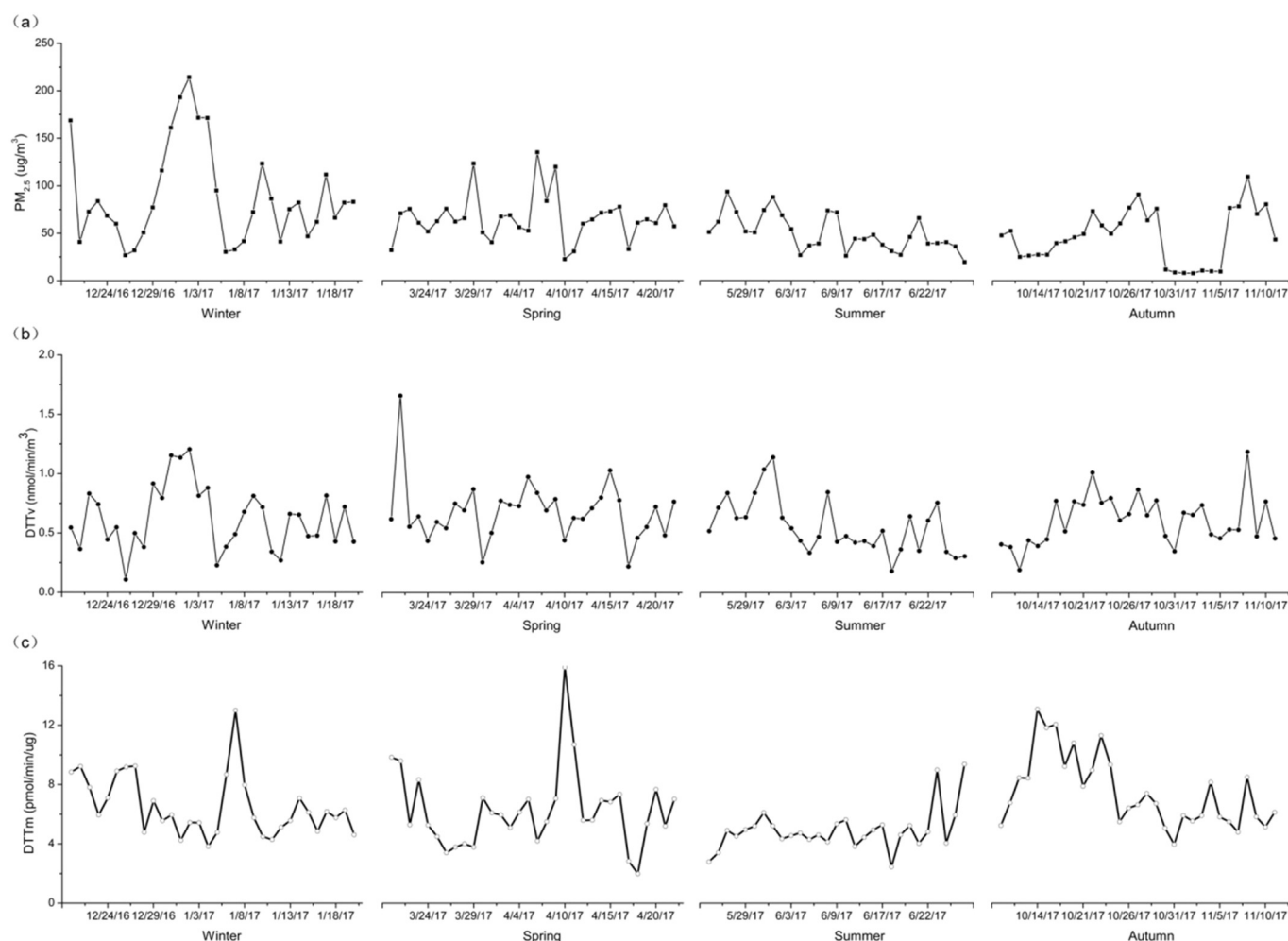Fig. 2. The averaged 48-hour air mass backward trajectories of Hangzhou city in 2017.

Fig. 3. Seasonal variations in daily PM$_{2.5}$ concentrations (a) with the corresponding water-soluble oxidative potential (b:DTTv; c:DTTm).

strong seasonality (p = 0.002) and ranked as autumn (average: 7.50, median: 6.73, range: 3.97–13.08 pmol/min/μg) > winter (average: 6.53, median: 5.95, range: 3.83–13.01 pmol/min/μg) > spring (average: 6.49, median: 5.77, range: 1.99–22.70 pmol/min/μg) > summer (average: 4.92, median: 4.74, range: 2.45–9.37 pmol/min/μg), indicating that the DTT-active components changed in different seasons. DTT activities were much higher in autumn and winter, and the lowest in summer, in line with the other reported sites (Saffari et al., 2014; Verma et al., 2014). A possible explanation is that the redox-active components (e.g. volatile and semivolatile organic compounds) are produced increasingly during the heating period for the fuel combustion (Biswas et al., 2009; Ntziachristos et al., 2007; Verma et al., 2011).

3.3. The diurnal variation trend of DTTv and DTTm

To identify diurnal variability of particulate OP, the sequence diagrams of DTTv and DTTm during summer day and night and autumn day and night were plotted (Fig. 4). The DTTv and DTTm in summer was basically consistent and had no significant diurnal variations (Fig. 4a, c). A previous report conducted in Bohai Sea showed significantly higher DTTv and DTTm in summer nighttime than in daytime (nighttime-to-daytime ratios for DTTv: 1.4; for DTTm: 1.9) (Liu et al., 2018). Our results are affected to some extent by the diurnal ambiguous demarcation. More evidence suggested that changes in composition contribute to the diurnal variation. In autumn, the similar tendency was also observed in DTTv (Fig. 4b, d). However, the DTTm in autumn was significantly higher in nighttime than in

daytime, indicating substantial DTT-active components existed at autumn night.

We further analyzed the corresponding components in term of Day/Night ratios (Fig. 5) and recorded the diurnal averaged concentrations of components (Table S1). NO$_3^-$ and NH$_4^+$ showed similar diurnal patterns with relatively higher concentrations occurred in summer daytime than in nighttime, however, relatively higher concentrations were detected in autumn nighttime than in daytime. This observation is in line with the reported investigation (Galindo and Yubero, 2017; Jalava et al., 2015), indicating that the thermal decomposition of particulate NH$_4$NO$_3$ may partly contribute to the source of nitrate and ammonium salt. The meteorological conditions may also affect the temporal distribution of components. SO$_4^{2-}$ exhibited higher concentrations in daytime than in nighttime at both seasons, indicating that the photochemical process of SO$_2$ to sulphate was enhanced under relatively higher temperature and intense sunshine conditions during daytime (Ye et al., 2017). We found that the dominance of SIA in ambient PM$_{2.5}$ appeared to relatively reduce DTTm, in line with reported relationship between SIA species and DTT activity of ambient fine aerosol in Indo-Gangetic plain (Patel and Rastogi, 2018). Additionally, the temporal patterns of Cl$^-$, Na$^+$ and K$^+$ were usually affected by the sea-land breeze circulation and biomass combustion sources, while Ca^{2+} and Mg^{2+} were influenced by the road dust resuspension (Fushimi et al., 2017). Various atmospheric chemical reactions dominated by photocatalytic process changed chemical properties of ambient particulate components such as the DTT activity.
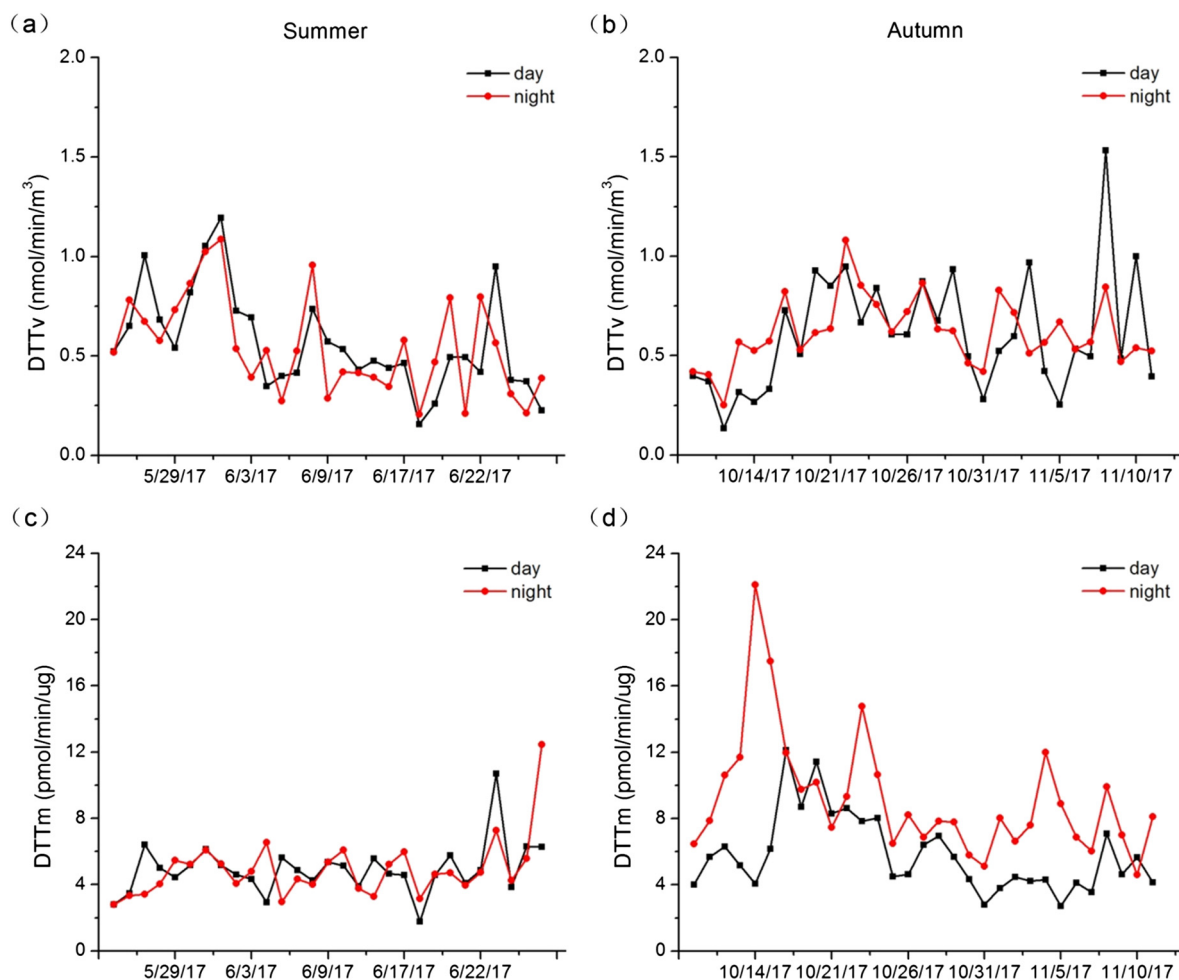
Fig. 4. The sequence diagrams of volume-normalized DTT activity and mass-normalized DTT activity during summer day and night (a and c, respectively) and autumn day and night (b and d, respectively).

3.4. The correlation of PM components with DTT activity

To investigate the components responsible for observed OP, the DTTv was linearly regressed against the measured water-soluble components. Most of the components at day or at night in summer (Fig. 6)
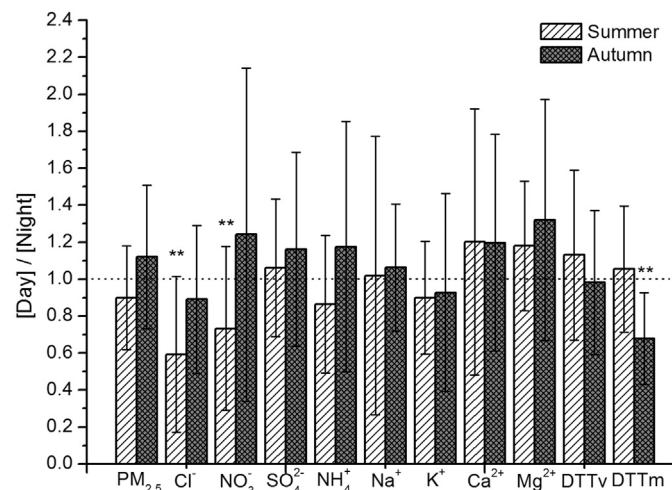

Fig. 5. Averaged diurnal ratios of $PM_{2.5}$, chemical components and DTT activities during summer (a) and autumn (b). Error bar indicates SD of average and Day/Night significantly different from 1: *p < 0.05, **p < 0.01.

and autumn (Fig. 7) showed positive correlation with DTTv. There was a greater relevance and steeper slope during day than during night, indicating that the components are more likely to affect DTT activity in daytime meteorological conditions.

The $PM_{2.5}$ mass concentration was correlated with the corresponding DTTv. The values of $r_s > 0.7$, $0.5 < r_s < 0.7$ and $r_s < 0.5$ indicate strong correlation, moderate correlation and weak correlation, respectively. It showed significant diurnal variations with strong or close to strong correlations at day (summer: $r_s = 0.834$; autumn: $r_s = 0.691$) and weak correlations at night (summer: $r_s = 0.334$; autumn: $r_s = 0.274$). This diurnal variation may be due to the changes in chemical properties of components under different meteorological conditions. Additionally, Ca^{2+} and Mg^{2+} only showed significant correlations with DTTv in autumn day ($r_s = 0.486$ and 0.586, respectively), indicating that road dust resuspension plays nonnegligible roles in the contribution of DTT activity.

Although SIA was reported to be DTT-inactive (Patel and Rastogi, 2018), it was produced along with the formation of secondary organic species, which had synergistic contribution to the OP of $PM_{2.5}$ (Verma et al., 2009). Secondary aerosol formation was significantly contributed to the associated DTT activity (Ma et al., 2018), therefore the relation of SIA to exposure-relevant DTT activity cannot be ignored. SIA species showed strong correlations (except NO_3^- during summer) with DTTv during day and weak correlations during night (Figs. 6, c, d and 7, b, c, d), indicating that strong secondary formation in daytime were contributed to the particulate OP. The strong correlations between SIA species and DTT activity indicated that there is a SIA-relevant oxidation risk. The sulfate partly contributes to the production of highly acidic aerosols and
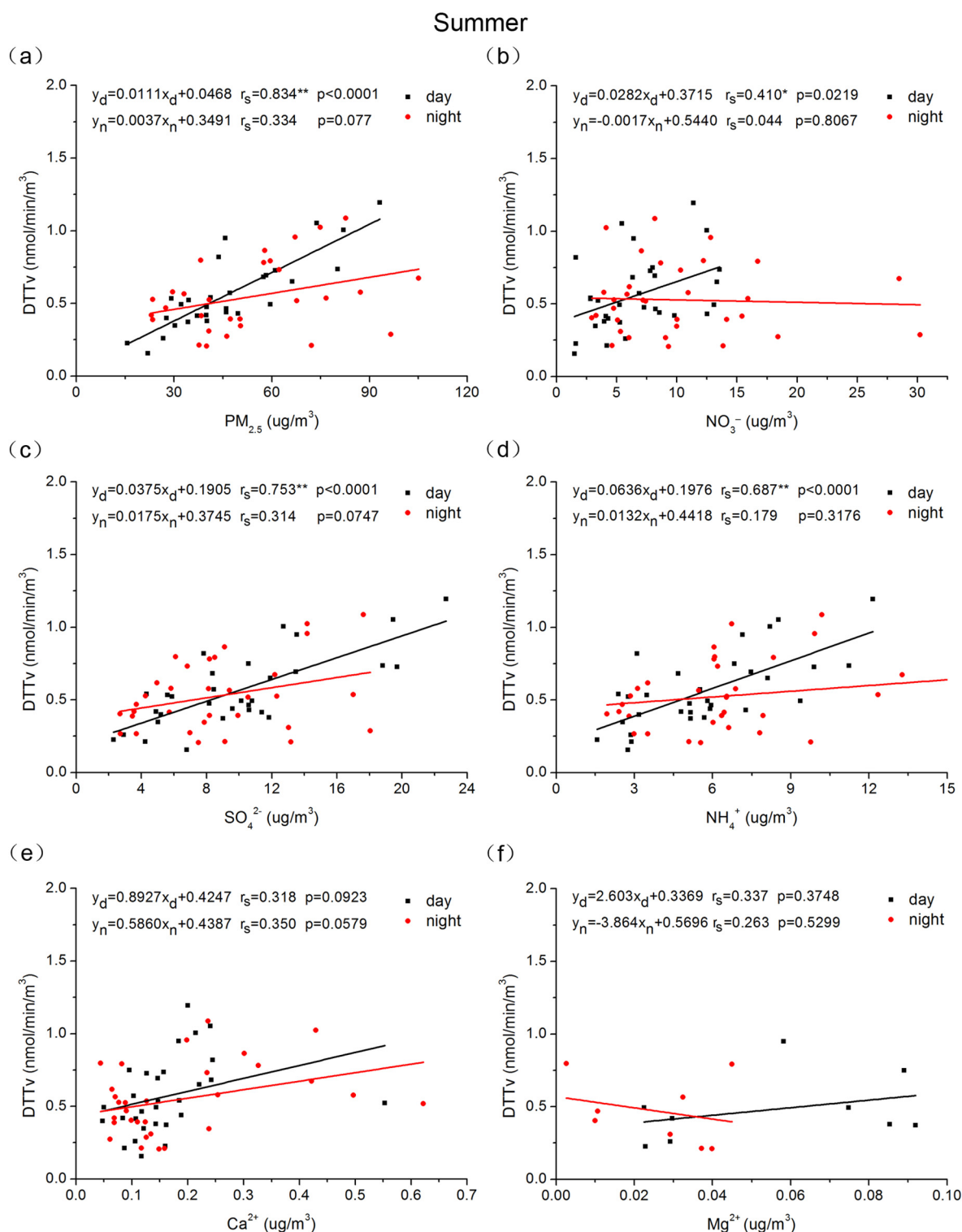
Summer

Fig. 6. Spearman correlation between DTTv and water-soluble ion components during summer day and night. The symbol * stands for a significant correlation (*p < 0.05, **p < 0.01).

was reported to improve particulate OP and sulfate-health relation risks (Fang et al., 2017a; Yu et al., 2018). The evaluation of PM components rather than mass concentration is thus more responsible for relevant risk assessment.

4. Conclusions

Our measurement of $PM_{2.5}$ in Hangzhou city in 2017 showed the seasonal variation of $PM_{2.5}$ concentrations. The observed relatively

higher DTTv and lower DTTm suggested a relatively high exposure risk and low intrinsic oxidative toxicity for ambient $PM_{2.5}$. The minimum of DTT activities occurred in summer and the remarkable seasonal variations might be related to the low emissions and the conversion of active components under high temperature environment. No obvious diurnal differences of DTT activities were found except the values of DTTm during autumn, indicating that the DTT-active components were changed. The $PM_{2.5}$ mass concentration was more significantly associated with DTTv during day than during

Autumn

（a）

$y_d=0.0064x_d+0.3047$ $r_s=0.691**$ $p<0.0001$
$y_n=0.0017x_n+0.5392$ $r_s=0.274$ $p=0.1356$

■ day
● night

(DTTv (nmol/min/m³) vs PM$_{2.5}$ (ug/m³))

（b）

$y_d=0.0275x_d+0.2801$ $r_s=0.812**$ $p<0.0001$
$y_n=0.0176x_n+0.4324$ $r_s=0.527**$ $p=0.0023$

■ day
● night

(DTTv (nmol/min/m³) vs NO$_3^-$ (ug/m³))

（c）

$y_d=0.0450x_d+0.2635$ $r_s=0.708**$ $p<0.0001$
$y_n=0.0249x_n+0.4448$ $r_s=0.444*$ $p=0.0123$

■ day
● night

(DTTv (nmol/min/m³) vs SO$_4^{2-}$ (ug/m³))

（d）

$y_d=0.0593x_d+0.2451$ $r_s=0.806**$ $p<0.0001$
$y_n=0.0332x_n+0.4324$ $r_s=0.483**$ $p=0.0060$

■ day
● night

(DTTv (nmol/min/m³) vs NH$_4^+$ (ug/m³))

（e）

$y_d=1.1620x_d+0.3500$ $r_s=0.486**$ $p=0.0065$
$y_n=0.2157x_n+0.5672$ $r_s=0.192$ $p=0.2998$

■ day
● night

(DTTv (nmol/min/m³) vs Ca^{2+} (ug/m³))

（f）

$y_d=4.4370x_d+0.3251$ $r_s=0.586**$ $p=0.0005$
$y_n=1.5480x_n+0.5325$ $r_s=0.283$ $p=0.1231$

■ day
● night

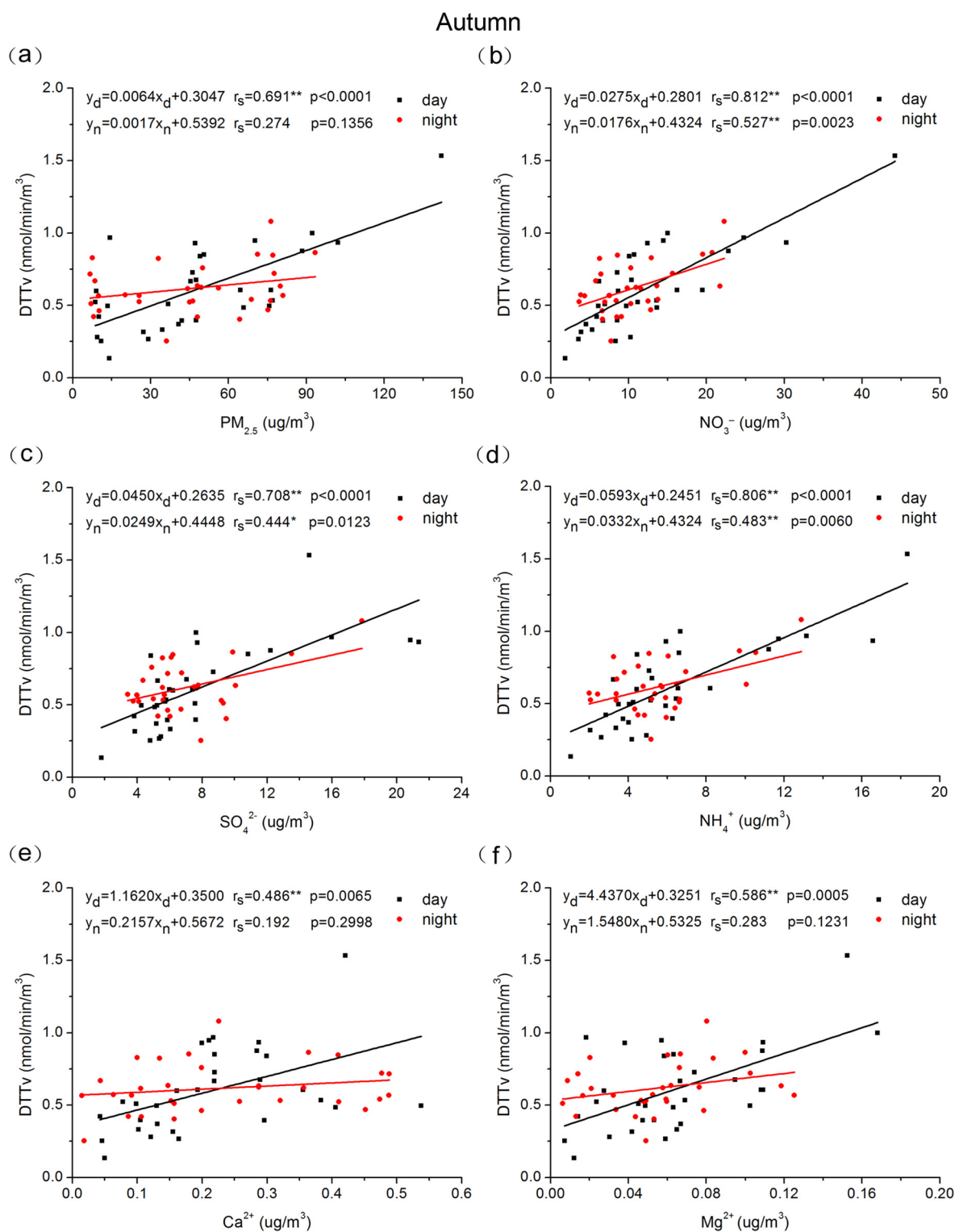(DTTv (nmol/min/m³) vs Mg^{2+} (ug/m³))

Fig. 7. Spearman correlation between DTTv and water-soluble ion components during autumn day and night. The symbol * stands for a significant correlation (*p < 0.05, **p < 0.01).

night, suggesting that the PM components rather than mass concentration are more responsible for the particulate OP. Future risk assessment of PM toxicity should fully consider both the mass concentration and its internal components of PM. SIA species were the dominant components of PM$_{2.5}$ (accounted for >50% of PM$_{2.5}$ concentration) and were correlated well with DTTv, indicating a higher SIA-relevant exposure risk. Our results will be beneficial for the evaluation of the important role of PM$_{2.5}$ components on adverse health effects.

Competing interests

The authors declare no competing financial interest.

Appendix A. Supplementary data

Supplementary data to this article can be found online at https://doi.org/10.1016/j.scitotenv.2018.08.375.

References

Abrams, J.Y., Weber, R.J., Klein, M., Samat, S.E., Chang, H.H., Strickland, M.J., Verma, V., Fang, T., Bates, J.T., Mulholland, J.A., Russell, A.G., Tolbert, P.E., 2017. Associations between ambient fine particulate oxidative potential and cardiorespiratory emergency department visits. Environ. Health Perspect. 125 (10) (UNSP 107008).

Bates, J.T., Weber, R.J., Abrams, J., Verma, V., Fang, T., Klein, M., Strickland, M.J., Sarnat, S.E., Chang, H.H., Mulholland, J.A., Tolbert, P.E., Russell, A.G., 2015. Reactive oxygen species generation linked to sources of atmospheric particulate matter and cardiorespiratory effects. Environ. Sci. Technol. 49 (22), 13605–13612.

Becker, S., Dailey, L.A., Soukup, J.M., Grambow, S.C., Devlin, R.B., Huang, Y.C.T., 2005. Seasonal variations in air pollution particle-induced inflammatory mediator release and oxidative stress. Environ. Health Perspect. 113 (8), 1032–1038.

Biswas, S., Verma, V., Schauer, J.J., Cassee, F.R., Cho, A.K., Sioutas, C., 2009. Oxidative potential of semi-volatile and non volatile particulate matter (PM) from heavy-duty vehicles retrofitted with emission control technologies. Environ. Sci. Technol. 43 (10), 3905–3912.

Cao, J.J., Xu, H.M., Xu, Q., Chen, B.H., Kan, H.D., 2012. Fine particulate matter constituents and cardiopulmonary mortality in a heavily polluted Chinese city. Environ. Health Perspect. 120 (3), 373–378.

Charrier, J.G., Anastasio, C., 2012. On dithiothreitol (DTT) as a measure of oxidative potential for ambient particles: evidence for the importance of soluble transition metals. Atmos. Chem. Phys. 12 (19), 9321–9333.

Chirizzi, D., Cesari, D., Guascito, M.R., Dinoi, A., Giotta, L., Donateo, A., Contini, D., 2017. Influence of Saharan dust outbreaks and carbon content on oxidative potential of water-soluble fractions of $PM_{2.5}$ and PM_{10}. Atmos. Environ. 163, 1–8.

Cho, A.K., Sioutas, C., Miguel, A.H., Kumagai, Y., Schmitz, D.A., Singh, M., Eiguren-Fernandez, A., Froines, J.R., 2005. Redox activity of airborne particulate matter at different sites in the Los Angeles Basin. Environ. Res. 99 (1), 40–47.

Cohen, A.J., Brauer, M., Burnett, R., Anderson, H.R., Frostad, J., Estep, K., Balakrishnan, K., Brunekreef, B., Dandona, L., Dandona, R., Feigin, V., Freedman, G., Hubbell, B., Jobling, A., Kan, H., Knibbs, L., Liu, Y., Martin, R., Morawska, L., Pope, C.A., Shin, H., Straif, K., Shaddick, G., Thomas, M., van Dingenen, R., van Donkelaar, A., Vos, T., Murray, C.J.L., Forouzanfar, M.H., 2017. Estimates and 25-year trends of the global burden of disease attributable to ambient air pollution: an analysis of data from the Global Burden of Diseases Study 2015. Lancet 389 (10082), 1907–1918.

Crobeddu, B., Aragao-Santiago, L., Bui, L.C., Boland, S., Squiban, A.B., 2017. Oxidative potential of particulate matter 2.5 as predictive indicator of cellular stress. Environ. Pollut. 230, 125–133.

Fang, T., Guo, H., Verma, V., Peltier, R.E., Weber, R.J., 2015a. $PM_{2.5}$ water-soluble elements in the southeastern United States: automated analytical method development, spatiotemporal distributions, source apportionment, and implications for heath studies. Atmos. Chem. Phys. 15 (20), 11667–11682.

Fang, T., Verma, V., Guo, H., King, L.E., Edgerton, E.S., Weber, R.J., 2015b. A semi-automated system for quantifying the oxidative potential of ambient particles in aqueous extracts using the dithiothreitol (DTT) assay: results from the Southeastern Center for Air Pollution and Epidemiology (SCAPE). Atmos. Meas. Tech. 8 (1), 471–482.

Fang, T., Verma, V., Bates, J.T., Abrams, J., Klein, M., Strickland, M.J., Sarnat, S.E., Chang, H.H., Mulholland, J.A., Tolbert, P.E., Russell, A.G., Weber, R.J., 2016. Oxidative potential of ambient water-soluble $PM_{2.5}$ in the southeastern United States: contrasts in sources and health associations between ascorbic acid (AA) and dithiothreitol (DTT) assays. Atmos. Chem. Phys. 16 (6), 3865–3879.

Fang, T., Guo, H.Y., Zeng, L.H., Verma, V., Nenes, A., Weber, R.J., 2017a. Highly acidic ambient particles, soluble metals, and oxidative potential: a link between sulfate and aerosol toxicity. Environ. Sci. Technol. 51 (5), 2611–2620.

Fang, T., Zeng, L.H., Gao, D., Verma, V., Weber, R.J., 2017b. Ambient size distributions and lung deposition of aerosol dithiothreitol-measured oxidative potential: contrast between soluble and insoluble particles. Environ. Sci. Technol. 51 (12), 6802–6811.

Fushimi, A., Saitoh, K., Hayashi, K., Ono, K., Fujitani, Y., Villalobos, A.M., Shelton, B.R., Takami, A., Tanabe, K., Schauer, J.J., 2017. Chemical characterization and oxidative potential of particles emitted from open burning of cereal straws and rice husk under flaming and smoldering conditions. Atmos. Environ. 163, 118–127.

Galindo, N., Yubero, E., 2017. Day-night variability of water-soluble ions in PM_{10} samples collected at a traffic site in southeastern Spain. Environ. Sci. Pollut. Res. 24 (1), 805–812.

Gao, D., Fang, T., Verma, V., Zeng, L.G., Weber, R.J., 2017. A method for measuring total aerosol oxidative potential (OP) with the dithiothreitol (DTT) assay and comparisons between an urban and roadside site of water-soluble and total OP. Atmos. Meas. Tech. 10 (8), 2821–2835.

Hystad, P., Demers, P.A., Johnson, K.C., Carpiano, R.M., Brauer, M., 2013. Long-term residential exposure to air pollution and lung cancer risk. Epidemiology 24 (5), 762–772.

Jalava, P., Wang, Q., Kuuspalo, K., Ruusunen, J., Hao, L., Fang, D., Vaisanen, O., Ruuskanen, A., Sippula, O., Happo, M., Uski, O., Kasurinen, S., Torvela, T., Koponen, H., Lehtinen, K., Komppula, M., Gu, C., Jokiniemi, J., Hirvonen, M.R., 2015. Day and night variation in chemical composition and toxicological responses of size segregated urban air PM samples in a high air pollution situation. Atmos. Environ. 120, 427–437.

Jansen, R.C., Shi, Y., Chen, J.M., Hu, Y.J., Xu, C., Hong, S.M., Jiao, L., Zhang, M., 2014. Using hourly measurements to explore the role of secondary inorganic aerosol in $PM_{2.5}$ during haze and fog in Hangzhou, China. Adv. Atmos. Sci. 31, 1427–1434.

Kumagai, Y., Arimoto, T., Shinyashiki, M., Shimojo, N., Nakai, Y., Yoshikawa, T., Sagai, M., 1997. Generation of reactive oxygen species during interaction of diesel exhaust particle components with NADPH-cytochrome P450 reductase and involvement of the bioactivation in the DNA damage. Free Radic. Biol. Med. 22, 479–487.

Kumagai, Y., Koide, S., Taguchi, K., Endo, A., Nakai, Y., Yoshikawa, T., Shimojo, N., 2002. Oxidation of proximal protein sulfhydryls by phenanthraquinone, a component of diesel exhaust particles. Chem. Res. Toxicol. 15 (4), 483–489.

Li, L., An, J.Y., Zhou, M., Yan, R.S., Huang, C., Lu, Q., Lin, L., Wang, Y.J., Tao, S.K., Qiao, L.P., Zhu, S.H., Chen, C.H., 2015. Source apportionment of fine particles and its chemical components over the Yangtze River Delta, China during a heavy haze pollution episode. Atmos. Environ. 123, 415–429.

Liu, Q.Y., Baumgartner, J., Zhang, Y.X., Liu, Y.J., Sun, Y.J., Zhang, M.G., 2014. Oxidative potential and inflammatory impacts of source apportioned ambient air pollution in Beijing. Environ. Sci. Technol. 48 (21), 12920–12929.

Liu, H.J., Xia, Y.L., Cai, W.D., Zhang, Y.N., Zhang, X.Q., Du, S.T., 2017. Enantioselective oxidative stress and oxidative damage caused by Rac- and S-metolachlor to *Scenedesmus obliquus*. Chemosphere 173, 22–30.

Liu, W.J., Xu, Y.S., Liu, W.X., Liu, Q.Y., Yu, S.Y., Liu, Y., Wang, X., Tao, S., 2018. Oxidative potential of ambient $PM_{2.5}$ in the coastal cities of the Bohai Sea, northern China: seasonal variation and source apportionment. Environ. Pollut. 236, 514–528.

Lyu, Y., Guo, H., Cheng, T., Li, X., 2018. Particle size distributions of oxidative potential of lung-deposited particles: assessing contributions from quinones and water-soluble metals. Environ. Sci. Technol. 52 (11), 6592–6600.

Ma, Y.Q., Cheng, Y.B., Qiu, X.H., Cao, G., Fang, Y.H., Wang, J.X., Zhu, T., Yu, J.Z., Hu, D., 2018. Sources and oxidative potential of water-soluble humic-like substances (HULISws) in fine particulate matter ($PM_{2.5}$) in Beijing. Atmos. Chem. Phys. 18, 5607–5617.

Ntziachristos, L., Froines, J.R., Cho, A.K., Sioutas, C., 2007. Relationship between redox activity and chemical speciation of size-fractionated particulate matter. Part. Fibre. Toxicol. 4, 5.

Patel, A., Rastogi, N., 2018. Oxidative potential of ambient fine aerosol over a semi-urban site in the Indo-Gangetic Plain. Atmos. Environ. 175, 127–134.

Perrone, M.G., Zhou, J., Malandrino, M., Sangiorgi, G., Rizzi, C., Ferrero, L., Dommen, J., Bolzacchini, E., 2016. PM chemical composition and oxidative potential of the soluble fraction of particles at two sites in the urban area of Milan, Northern Italy. Atmos. Environ. 128, 104–113.

Pope, C.A., Burnett, R.T., Thurston, G.D., Thun, M.J., Calle, E.E., Krewski, D., Godleski, J.J., 2004. Cardiovascular mortality and long-term exposure to particulate air pollution - epidemiological evidence of general pathophysiological pathways of disease. Circulation 109 (1), 71–77.

Rattanavaraha, W., Rosen, E., Zhang, H.F., Li, Q.F., Pantong, K., Kamens, R.M., 2011. The reactive oxidant potential of different types of aged atmospheric particles: an outdoor chamber study. Atmos. Environ. 45 (23), 3848–3855.

Rui, W., Guan, L.F., Zhang, F., Zhang, W., Ding, W.J., 2016. $PM_{2.5}$-induced oxidative stress increases adhesion molecules expression in human endothelial cells through the ERK/AKT/NF-kappa B-dependent pathway. J. Appl. Toxicol. 36 (1), 48–59.

Saffari, A., Daher, N., Shafer, M.M., Schauer, J.J., Sioutas, C., 2014. Seasonal and spatial variation in dithiothreitol (DTT) activity of quasi-ultrafine particles in the Los Angeles Basin and its association with chemical species. J. Environ. Sci. Health A 49 (4), 441–451.

Soberanes, S., Urich, D., Baker, C.M., Burgess, Z., Chiarella, S.E., Bell, E.L., Ghio, A.J., De Vizcaya-Ruiz, A., Liu, J., Ridge, K.M., Kamp, D.W., Chandel, N.S., Schumacker, P.T., Mutlu, G.M., Budinger, G.R.S., 2009. Mitochondrial complex III-generated oxidants activate ASK1 and JNK to induce alveolar epithelial cell death following exposure to particulate matter air pollution. J. Biol. Chem. 284 (4), 2176–2186.

Sun, Q.H., Hong, X.R., Wold, L.E., 2010. Cardiovascular effects of ambient particulate air pollution exposure. Circulation 121 (25), 2755–2765.

Tuet, W.Y., Chen, Y.L., Xu, L., Fok, S., Gao, D., Weber, R.J., Ng, N.L., 2017. Chemical oxidative potential of secondary organic aerosol (SOA) generated from the photooxidation of biogenic and anthropogenic volatile organic compounds. Atmos. Chem. Phys. 17 (2), 839–853.

Valavanidis, A., Vlachogianni, T., Fiotakis, K., Loridas, S., 2013. Pulmonary oxidative stress, inflammation and cancer: respirable particulate matter, fibrous dusts and ozone as major causes of lung carcinogenesis through reactive oxygen species mechanisms. Int. J. Env. Res. Publ. Health 10 (9), 3886–3907.

Vattanasit, U., Navasumrit, P., Khadka, M.B., Kanitwithayanun, J., Promvijit, J., Autrup, H., Ruchirawat, M., 2014. Oxidative DNA damage and inflammatory responses in cultured human cells and in humans exposed to traffic-related particles. Int. J. Hyg. Environ. Health 217 (1), 23–33.

Verma, V., Ning, Z., Cho, A.K., Schauer, J.J., Shafer, M.M., Sioutas, C., 2009. Redox activity of urban quasi-ultrafine particles from primary and secondary sources. Atmos. Environ. 43 (40), 6360–6368.

Verma, V., Pakbin, P., Cheung, K.L., Cho, A.K., Schauer, J.J., Shafer, M.M., Kleinman, M.T., Sioutas, C., 2011. Physicochemical and oxidative characteristics of semi-volatile components of quasi-ultrafine particles in an urban atmosphere. Atmos. Environ. 45 (4), 1025–1033.

Verma, V., Fang, T., Guo, H., King, L., Bates, J.T., Peltier, R.E., Edgerton, E., Russell, A.G., Weber, R.J., 2014. Reactive oxygen species associated with water-soluble $PM_{2.5}$ in the southeastern United States: spatiotemporal trends and source apportionment. Atmos. Chem. Phys. 14 (23), 12915–12930.

Verma, V., Fang, T., Xu, L., Peltier, R.E., Russell, A.G., Ng, N.L., Weber, R.J., 2015. Organic aerosols associated with the generation of reactive oxygen species (ROS) by water-soluble $PM_{2.5}$. Environ. Sci. Technol. 49 (7), 4646–4656.

Vreeland, H., Weber, R., Bergin, M., Greenwald, R., Golan, R., Russell, A.G., Verma, V., Sarnat, J.A., 2017. Oxidative potential of $PM_{2.5}$ during Atlanta rush hour: measurements of in-vehicle dithiothreitol (DTT) activity. Atmos. Environ. 165, 169–178.

Wu, J., Xu, C., Wang, Q.Z., Cheng, W., 2016. Potential sources and formations of the $PM_{2.5}$ pollution in urban Hangzhou. Atmosphere 7 (8), 100.

Xu, J.S., Xu, M.X., Snape, C., He, J., Behera, S.N., Xu, H.H., Ji, D.S., Wang, C.J., Yu, H., Xiao, H., Jiang, Y.J., Qi, B., Du, R.G., 2017. Temporal and spatial variation in major ion chemistry and source identification of secondary inorganic aerosols in Northern Zhejiang Province, China. Chemosphere 179, 316–330.

Xu, F.F., Qiu, X.H., Hu, X.Y., Shang, Y., Pardo, M., Fang, Y.H., Wang, J.X., Rudich, Y.N., Zhu, T., 2018. Effects on IL-1 beta signaling activation induced by water and organic extracts of fine particulate matter ($PM_{2.5}$) in vitro. Environ. Pollut. 237, 592–600.

Ye, Z.L., Li, Q., Ma, S.S., Zhou, Q.F., Gu, Y., Su, Y.L., Chen, Y.F., Chen, H., Wang, J.F., Ge, X.L., 2017. Summertime day-night differences of $PM_{2.5}$ components (inorganic ions, OC, EC, WSOC, WSON, HULIS, and PAHs) in Changzhou, China. Atmosphere 8 (10), 189.

Yu, N.Y., Guo, H.W., Yang, J.P., Jin, L., Wang, X.B., Shi, W., Zhang, X.W., Yu, H.X., Wei, S., 2018. Non-target and suspect screening of per- and polyfluoroalkyl substances in airborne particulate matter in China. Environ. Sci. Technol. 52, 8205–8214.

Zhang, G., Xu, H.H., Qi, B., Du, R.G., Gui, K., Wang, H.L., Jiang, W.T., Liang, L.L., Xu, W.Y., 2018. Characterization of atmospheric trace gases and particulate matter in Hangzhou, China. Atmos. Chem. Phys. 18 (3), 1705–1728.